IVYSPRING INTERNATIONAL PUBLISHER

International Journal of Biological Sciences

2018; 14(4): 418-426. doi: 10.7150/ijbs.23602

Research Paper

Glaucocalyxin A induces G2/M cell cycle arrest and apoptosis through the PI3K/Akt pathway in human bladder cancer cells

Wenfeng Lin[1,2*], Jinlin Xie[1,2*], Naijin Xu[3], Linglong Huang[1,2], Abai Xu[1,2], Hulin Li[1,2], Chaoming Li[1,2], Yubo Gao[1,2], Masami Watanabe[3], Chunxiao Liu[1,2], Peng Huang[1,2,3,4]✉

1. Department of Urology, Zhujiang Hospital, Southern Medical University, Guangzhou, China
2. Key Laboratory of Inflammatory and Immunological Diseases in Guangzhou, Zhujiang Hospital, Southern Medical University, Guangzhou, China
3. Department of Urology, Okayama University Graduate School of Medicine, Dentistry and Pharmaceutical Sciences, Okayama, Japan
4. Okayama Medical Innovation Center, Okayama University, Okayama, Japan

* Contributed equally to this work.

✉ Corresponding author: Peng Huang, Department of Urology, Zhujiang Hospital of Southern Medical University, Guangzhou 510280, China; Tel: +86-20-62782725; E-mail:huangpeng509@gmail.com

Received: 2017.11.01; Accepted: 2018.02.18; Published: 2018.03.10

Abstract

Glaucocalyxin A (GLA), a major component isolated from Rabdosia japonica, has been proven to show anti-bacterial and anti-tumor biological characteristics according to previous studies. However, its potential effect on bladder cancer remains unknown. The present research aims to investigate the underlying mechanism in treating bladder cancer in vivo and in vitro. Cell proliferation was analyzed by CCK-8 assay and colony formation. Flow cytometry was used to measure the cell cycle distribution and apoptosis. The expressions of the cell cycle and apoptosis-related proteins were detected by western blotting and immunofluorescence staining. Meanwhile, the in vivo study was performed to evaluate the anti-tumor effect on a UMUC3 subcutaneous tumor of NOD/SCID mice model. GLA suppressed colony-formation ability, triggered G2/M arrest and promoted apoptosis of UMUC3 cells in a dose-dependent manner. Furthermore, western blotting showed that GLA downregulated the expressions of PI3K p85, p-Akt, Bcl-2, CDK1, Cyclin B1 whereas upregulated the levels of PTEN, Bax, Cleaved Caspase-3. In vivo, GLA at a dosage of 20 mg/kg significantly inhibited tumor growth compared with the control group by intraperitoneal injection. These results suggested that GLA-related G2/M arrest and apoptosis in UMUC3 cells were mediated by a suppressed PI3K/Akt signaling pathway, which regulated $p21^{Waf1/Cip1}$ as well as intrinsic caspase cascade. Collectively, our observations could help to develop new drugs targeting the PI3K/Akt pathway for the treatment of bladder cancer.

Key words: Glaucocalyxin A, bladder cancer, cell cycle, apoptosis, PI3K/Akt pathway

Introduction

GLA is a diterpenoid compound extracted and purified from the traditional Chinese herb, Rabdosia japonica (Burm.f.) Hara var. Glaucocalyx (Maxim.) Hara [1, 2]. Previous studies have reported that GLA possesses various biological characteristics against bacteria, oxidation, thrombosis, coagulation, and inflammation [3]. The anti-tumor effect has been explored in leukemia and several types of solid tumors. In human leukemia HL-60 cells, GLA-induced apoptosis is mediated by reactive oxygen species (ROS)-mitochondria pathway [4]. GLA has been found to cause G2/M phase arrest and cell apoptosis in human breast cancer cells via the activated FasL protein and c-Jun N-terminal kinase (JNK) pathway [5]. The study about anti-glioma activity proves that GLA is effective to increase the

apoptotic rate of human brain glioblastoma U87MG cells as a negative Akt regulator [6]. *In vivo*, the anti-tumor effect is enhanced with GLA nanosuspensions (10 mg/kg) injected intravenously into hepatic tumor-bearing mice [7]. These findings above reveal that GLA may have promising therapeutic implications for some certain tumors. However, to our knowledge, there has been no research focusing on its anti-neoplastic activity against urinary carcinoma.

Urinary bladder cancer is the second most common urinary malignancy in the United States. It has been estimated that there would be 79,030 new cases of bladder cancer and that 16,870 patients will die of this disease in 2017 [8]. Of the newly diagnosed bladder cancer patients, about 75% are non-muscle-invasive bladder cancer (NMIBC). The 5-year recurrence rate reaches 50%-70% of NMIBC after transurethral resection, and the risk of 5-year progression ranges from 10% to 30% [9]. Although fewer patients are newly diagnosed with muscle-invasive bladder cancer (MIBC), they are responsible for the vast majority of bladder cancer-specific deaths [10]. Furthermore, the etiology and mechanism of bladder cancer remain unclear, leading to poor treatment results and heavy economic burden [11].

Therefore, this study was designed to explore the anti-tumor characteristics and the possible molecular mechanisms of GLA in human bladder cancer cells. Our data showed that GLA negatively regulated the phosphoinositide 3-kinase (PI3K)/Akt signaling pathway in UMUC3 cells. The downstream $p21^{Waf1/Cip1}$ and mitochondrial-mediated pathway led to cell cycle arrest at G2/M phase and apoptosis. Taken together, these findings give another perspective in the development of PI3K pathway targeted agents to treat bladder cancer.

Material and Methods

Chemicals and antibodies

GLA was purchased from Shanghai Yuanye Bio-Technology Company (Shanghai, China) and the molecular structure is shown in Fig. 1A. GLA was dissolved in dimethyl sulfoxide (DMSO) and filtered through a 0.22-mm filter (Millipore, USA) with a stock solution of 5 mM stored at -20 °C. The final DMSO concentration of working solution was less than 0.1% (v/v). The primary antibodies against Akt, phospho-Akt (Ser473), B-cell lymphoma 2 (Bcl-2), Bcl-2-associated X protein (Bax), Caspase-9, Cleaved Caspase-9, Caspase-3, Cleaved Caspase-3, Poly (ADP-ribose) polymerase (PARP), Ki-67, CD31, β-actin were purchased from Cell Signaling Technology (CST, Beverly, MA, USA). Anti-$p21^{Waf1/Cip1}$ (p21), Anti-Cyclin B1, Anti-CDK1 (cyclin-dependent kinase 1), Anti-Cdc25C (cell division cycle 25 homolog c), Anti-PI3K p85 and Anti-PTEN (phosphatase and tensin homolog) were provided by Wanlei Biological Technology (Shenyang, China). The secondary antibody was horseradish peroxidase (HRP)-conjugated goat anti-rabbit antibody from CST.

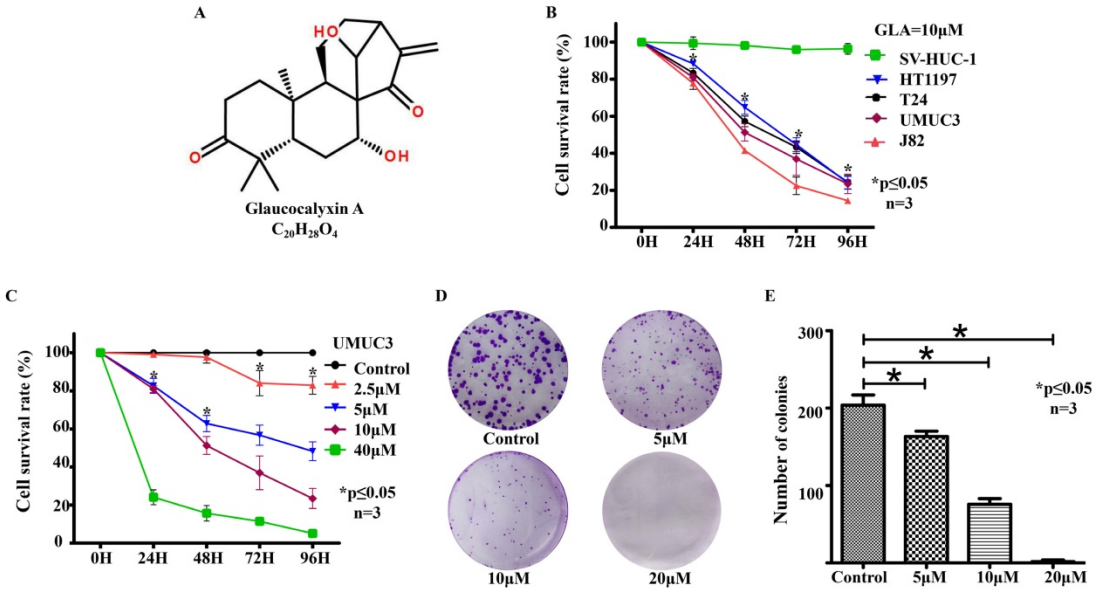

Figure 1. GLA inhibits cell proliferation and colony formation in human bladder cancer cell lines (A) The chemical structure of GLA. **(B)** The CCK-8 assay for UMUC3, HT1197, T24, J82 and SV-HUC-1 cells following treatment with 10 μM GLA for 96 h. **(C)** UMUC3 cells were treated with different concentrations of GLA (0, 2.5, 5, 10 or 40 μM) for 24, 48, 72, and 96 h. Cell viability was determined by the CCK-8 assay. **(D, E)** UMUC3 cells were treated with GLA (0, 5, 10 or 20 μM) and allowed to form colonies in fresh medium for 10 days. Photographic differences in colony formation and the number of colonies are shown. Data are expressed as the mean ± S.D. from three independent experiments. *$P < 0.05$ vs. the control group.

Cell and cell culture

Human bladder cancer cell lines UMUC3, HT1197, T24, J82 and human bladder epithelial cell line SV-HUC-1 were purchased from the Cell Bank of the Chinese Academy of Sciences (Shanghai, China). Cells were cultured in RPMI-1640 medium supplemented with 10% fetal bovine serum (FBS, Gibco, USA) and were incubated at 37 °C in a humidified atmosphere with 5% CO_2.

Cell viability assay

SV-HUC-1, HT1197, T24, J82, UMUC3 cells were seeded in 96-well plates at 5 × 10^3 per well and cultured for 24 h. The indicated concentrations of GLA were used to treat cells for 24, 48, 72 and 96 h. With an addition of Cell Counting Kit-8 (CCK-8) (10 µl per well), cells were then incubated at 37˚C for 1 h. The optical density (OD) levels were measured at 450 nm using the BioTek ELx808 Microplate Reader.

Colony formation assay

UMUC3 cells were seeded into six-well plates at a density of 500 cells per well and allowed to attach overnight. After treatment with 0, 5, 10 and 20 µM GLA respectively, these cells were continuously incubated in a humidified atmosphere of 5% CO_2 at 37 °C for 10 days. Visible colonies were fixed in 4% paraformaldehyde for 15 min and stained with 0.1% crystal violet for 30 min before gently washed twice in PBS. The plates were dried at room temperature and colonies containing over 50 cells were microscopically counted.

Cell Cycle Analysis

UMUC3 cells were seeded in six-well plates at a density of 2 × 10^5 cells per well. The next day, cells were treated with GLA (0, 5, 10 or 20 µM) for 24 h at 37˚C. For cell cycle analysis, cells were then harvested, washed twice with PBS and fixed in 70% ethanol at 4˚C overnight. After 15 min incubation with 50 µl RNase A plus 450 µl propidium iodide (PI), cells were subject to cell cycle analysis using the FACScan flow cytometer (BD Biosciences, San Diego, CA, USA). The cell cycle distribution was analyzed by ModFit LT™ version 3.0 (Verity Software House, Toshan, ME, USA).

Annexin V-FITC/PI assays for apoptosis

UMUC3 cells were seeded in six-well plates at 2 × 10^5 cells per well. After 24 h treatment with GLA (0, 5, 10 or 20 µM), cells were collected, washed twice with PBS and then resuspended in 400 µl of Annexin V binding buffer. Following incubation with 5 µl of FITC-conjugated Annexin V and 5 µl of PI for 15 min in the dark at room temperature, apoptotic cells were analyzed by FACScan flow cytometer and BD FACSuite™ software.

Western blot analysis

UMUC3 cells were washed twice with pre-cold PBS after 24 hours of treatment with 0, 20 and 40 µM GLA. The total proteins were extracted using RIPA lysis buffer plus Protease Inhibitor Cocktail and then quantified by BCA Protein Assay Kit (CWBiotech, Beijing, China). Equal amounts of proteins (30µg/ well) were subjected to 10% or 12% SDS-PAGE and then electrotransferred onto 0.45 µm PVDF membranes (Millipore, Billerica, MA, USA). The membranes were blocked with 5% non-fat milk or bovine serum albumin for 2 h at room temperature followed by overnight incubation in primary antibodies as described above at 4 °C. After washing with 1X TBS-T, the membranes were incubated with the indicated HRP-conjugated secondary antibodies for 1 h at room temperature. Proteins visualization was performed using the Chemiluminescent HRP Substrate (Millipore, Billerica, MA, USA) and the ChemiDoc™ XRS system (Bio-Rad, Hercules, CA, USA). β-actin was used as an internal control.

Immunofluorescence staining

UMUC3 cells were plated on 35 mm glass-bottom culture dishes. After 24 h treatment with GLA (0, 20 µM), cells were fixed with 4% paraformaldehyde for 15 min. The fixed cells were permeabilized with 0.5% Triton X-100 for 10 min and blocked with 10% normal goat serum for 30 min. Then cells were incubated with the primary antibodies against p-Akt (1:100) and Cleaved Caspase-3 (1:400) at 4°C overnight. After rinsing with PBS in triplicate for 5 min, cells were incubated with the fluorescent-labeled secondary antibody in the dark for 1 h. Finally, the nuclei were counterstained with DAPI followed by examination and photography using a Zeiss fluorescence microscope.

Animals

Six-week-old female non-obese diabetic/severe combined immunodeficient (NOD/SCID) mice were obtained from Japan SLC, Inc. (Hamamatsu, Japan) and were acclimated for 2 weeks. Mice were maintained in specific pathogen-free (SPF) conditions and provided with sterilized food and water in the Laboratory Animal Center of Okayama University. The protocols for animal experimentation were approved by the Okayama University Animal Research Committee.

Subcutaneous Tumor xenograft model

UMUC3 cells (1×10^6) were resuspended in 100 µl PBS with 50% of matrigel (BD Biosciences, CA,

USA) and then subcutaneously inoculated into the right rear flank of mice. When the tumor volume reached approximately 100 mm^3, tumor-bearing mice were randomized into two groups (nine mice per group) and assigned to intraperitoneally receive vehicle (PBS) or GLA (20 mg/kg) twice every three days for 2 weeks prior to sacrifice. The tumor volume was measured with a caliper every 4 days using the formula: (volume = $width^2$ × length × 0.52). At the endpoint, the tumors were surgically removed, weighed and photographed.

Immunohistochemical detection

Tumor tissues were fixed with 10% formaldehyde, embedded in paraffin and cut into 4 μm sections. After deparaffinized with xylene, sections were hydrated in descending series of ethanol. Subsequently, the endogenous peroxidase activity was reduced with 0.3% H_2O_2 for 10 min followed by antigen retrieval heated in 0.01 M citrate buffer for 4 min twice. Non-specific binding was blocked with serum for 30 min and sections were incubated with primary antibodies against Ki-67 (1:100) and CD31 (1:100) at 4 °C overnight. Following incubation with a biotinylated secondary antibody for 30 min at 37 °C, antibody binding was visualized by 3,3-diaminobenzidine (DAB) staining. The slides were counterstained with hematoxylin and observed under a Zeiss microscope.

Statistical analysis

Each experiment was repeated at least three times and data are shown as the mean ± standard deviation (S.D.). Statistical analyses were performed by SPSS software version 20.0 (SPSS Inc., Chicago, IL, USA). Between-group differences were estimated with one-way analysis of variance (ANOVA). A p value < 0.05 was considered to be statistically significant.

Results

GLA inhibits cell proliferation and colony formation in human bladder cancer cells.

To evaluate the effect of GLA, bladder cancer cell lines UMUC3, HT1197, T24, J82 and epithelial cell line SV-HUC-1 were treated with different concentrations of GLA (0, 2.5, 5, 10 or 40 μM) for 24, 48, 72, and 96 h. As shown in Fig. 1B, inhibition was observed in a time-dependent inhibition manner following treatment with 10 μM GLA in these bladder cancer cell lines. In the SV-HUC-1 cells, no statistical change was observed after each treatment. And GLA inhibited the viability of UMUC3 cells in a time- and dose-dependent manner (Fig. 1C). The IC50 values of GLA on UMUC3 cells at 24, 48, 72, and 96 h were 18.87, 9.77, 6.75, and 5.40 μM, respectively. The anti-proliferation effect of GLA on UMUC3 cells was further confirmed using colony formation assay. GLA significantly suppressed colony formation with a decreased number and size of cell colonies in a dose-dependent manner compared with the control group (Fig. 1(D, E)).

GLA triggers cell cycle arrest at the G2/M phase in UMUC3 cells.

To determine whether GLA inhibits the cell cycle progression, we treated UMUC3 cells with different concentrations of GLA for 24 h and then analyzed the cell cycle distribution by flow cytometry (Fig. 2A). After 24 hours, we observed that with higher concentration, more cells stayed in G2/M phase rather than G0/G1 and no significant difference in S phase, which indicates GLA seems to cause a G2/M phase arrest in UMUC3 cells (Figure 2B). Hence, we further assessed the molecular mechanism underlying GLA-induced cell cycle arrest in UMUC3 cells. The G2/M-related proteins were measured by western blotting. Fig. 2(C, D) showed GLA upregulated the expression level of $p21^{Waf1/Cip1}$ but downregulated Cyclin B1, CDK1, and Cdc25C. These results above indicate that GLA triggered G2/M phase arrest of UMUC3 cells in a dose-dependent manner.

GLA induces mitochondrial-mediated apoptosis of UMUC3 cells.

UMUC3 cells were treated with different concentrations of GLA (0, 5, 10, and 20 μM) for 24 h and were analyzed by flow cytometry (Fig. 3A). As shown in Fig. 3B, the apoptotic rates in GLA groups were 10.16 ± 1.10%, 29.99 ± 8.55%, and 53.61 ± 5.11% of the total cells respectively, compared with only 4.37 ± 1.17% in control group. Next, we detected the expression of proteins associated with the mitochondrial apoptotic pathway after GLA treatment (Fig. 3C). Western blotting analysis demonstrated that GLA increased Bax levels but decreased Bcl-2 levels as compared to control cells, leading to upregulation of the Bax/Bcl-2 ratio in a dose-dependent manner (Fig. 3D). Furthermore, the levels of Caspase-9, Caspase-3 and PARP decreased following GLA treatment with a corresponding significant accumulation of Cleaved Caspase-9, Cleaved Caspase-3 and Cleaved PARP (Fig. 3E). Meanwhile, immunofluorescence staining indicated that both cytoplasmic and nuclear expressions of Cleaved Caspase-3 were significantly enhanced after treatment with GLA (Fig. 4B). Our results suggest that GLA-induced apoptosis in UMUC3 cells was mediated through the intrinsic apoptotic pathway.

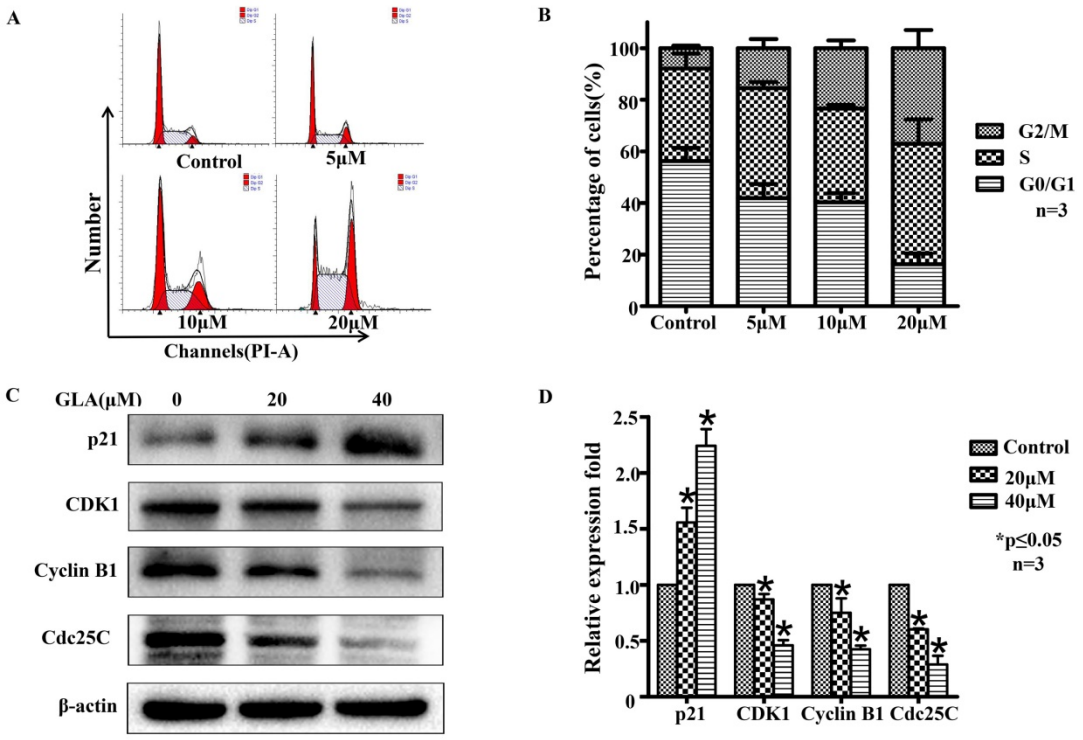

Figure 2. GLA triggers cell cycle arrest at the G2/M phase in UMUC3 cells. (A) UMUC3 cells were treated with indicated concentrations of GLA (0, 5, 10 and 20 μM) for 24 h. The harvested cells were then incubated with RNase A and PI. The cell cycle distribution was analyzed by flow cytometry. **(B)** The percentages of cells in G0/G1, S and G2/M phases are presented in the histograms. **(C, D)** UMUC3 cells were treated with GLA (0, 20 and 40 μM) for 24 h. Proteins were extracted and the expressions of $p21^{Waf1/Cip1}$, Cyclin B1, CDK1 and Cdc25C were then analyzed by western blotting. β-actin was used as a loading control. Data are expressed as the mean ± S.D. from three independent experiments. *P < 0.05 vs. the control group.

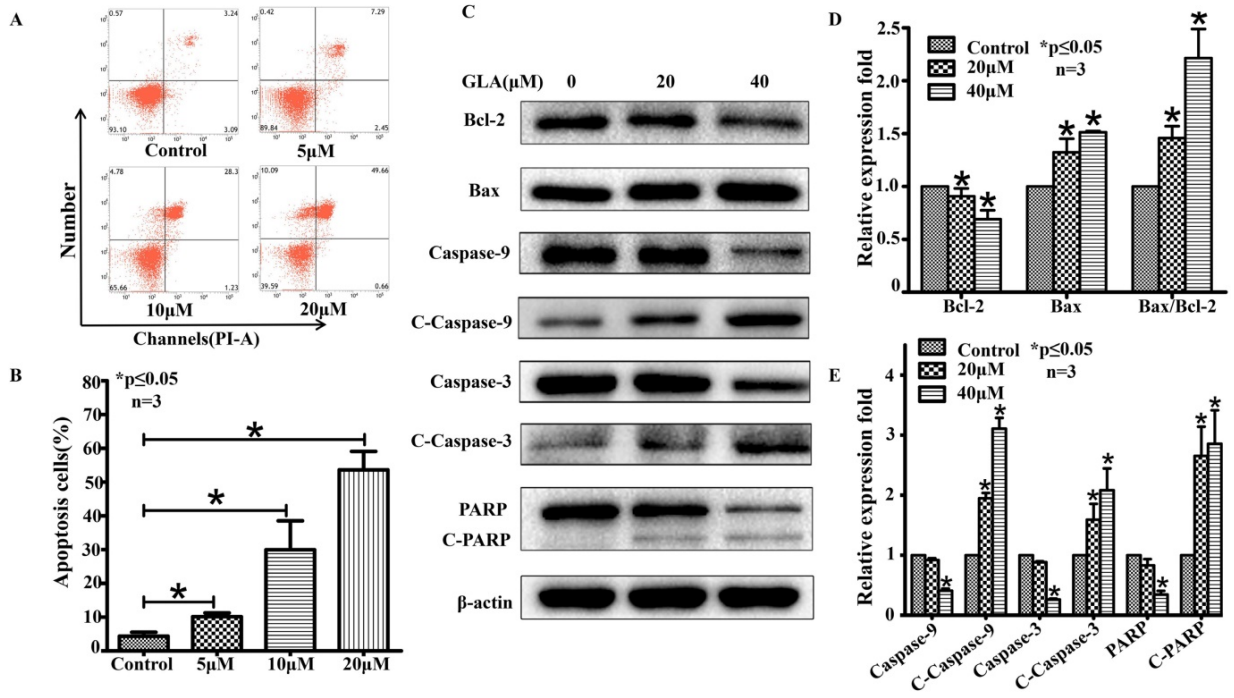

Figure 3. GLA induces mitochondrial-mediated apoptosis of UMUC3 cells. (A) UMUC3 cells were treated with various concentrations of GLA (0, 5, 10 and 20 μM) for 24 h. The harvested cells were then stained with Annexin V/PI and flow cytometry was performed to analyze apoptotic rates. **(B)** The histograms show the percentages of apoptotic cells. **(C-E)** UMUC3 cells were treated with GLA (0, 20 and 40 μM) for 24 h. Proteins were extracted and western blotting was then performed to analyze the expressions of Bax, Bcl-2, Caspase-9, Cleaved Caspase-9, Caspase-3, Cleaved Caspase-3, PARP and Cleaved PARP. The Bax/Bcl-2 ratio was also calculated as shown in the histogram. Data are expressed as the mean ± S.D. from three independent experiments. *P < 0.05 vs. the control group.

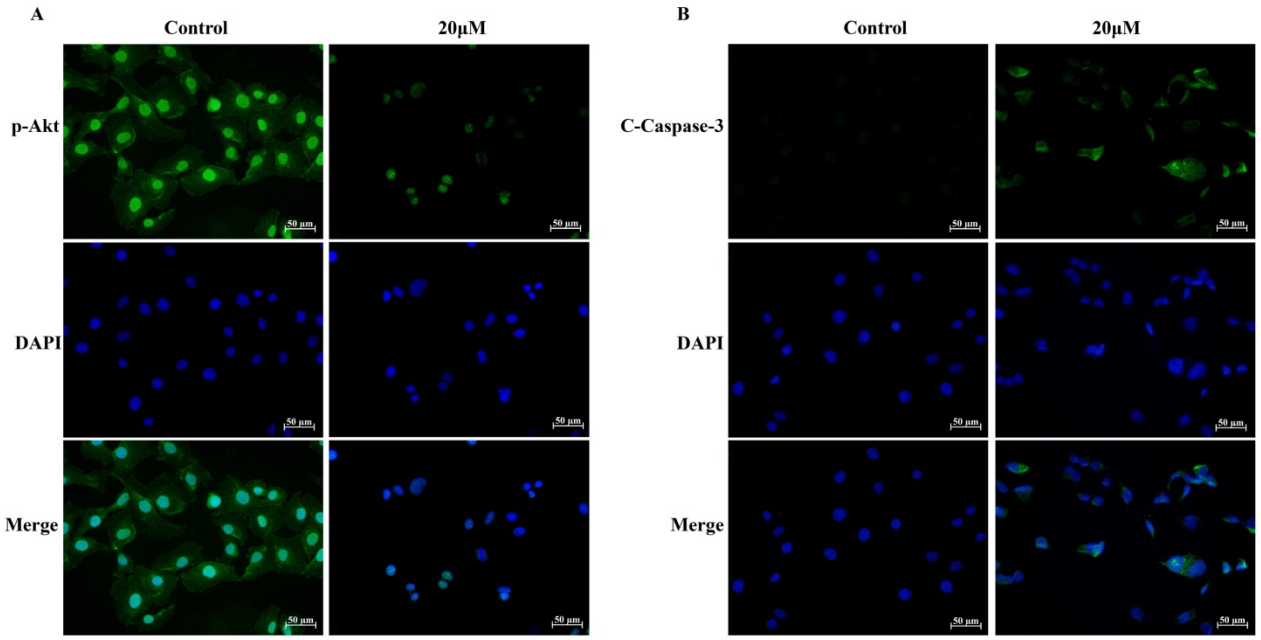

Figure 4. Immunofluorescence analysis for p-Akt (Ser473) and Cleaved Caspase-3. (A) The expression and location of p-Akt (Ser473) in UMUC3 cells treated with 0 or 20 μM GLA were detected by immunofluorescence staining (green) whereas the nuclei were stained with DAPI (blue). **(B)** The expression and location of Cleaved Caspase-3 in UMUC3 cells treated with 0 or 20 μM GLA were confirmed by immunofluorescence staining (green) whereas the nuclei were stained with DAPI (blue). Scale bars = 50 μm.

GLA inhibits the PI3K/Akt pathway in UMUC3 cells.

To explore the molecular mechanism of GLA-mediated apoptosis and G2/M arrest, we examined the expression of proteins associated with the PI3K/Akt pathway. Fig. 5(A, B) illustrates that GLA significantly decreased the levels of PI3K p85 subunit and the phosphorylation of Akt at Ser473 site, while the levels of PTEN increased in a dose-dependent manner. There was no significant difference in the expression of total Akt. The accumulation of the $p21^{Waf1/Cip1}$ and Bax proteins, which subsequently activated the downstream signaling involved in the regulation of G2/M arrest and apoptosis. Furthermore, decreased expressions of p-Akt (Ser473) were confirmed both in the cytoplasm and nuclear by immunofluorescence staining (Fig. 4A). Therefore, our data demonstrate that GLA suppressed the PI3K/Akt pathway in UMUC3 cells.

GLA exhibits the anti-tumor effect on UMUC3 cells in vivo.

To evaluate the anti-tumor effect of GLA in vivo, we established the UMUC3 tumor xenograft NOD/SCID mice model. The representative change of tumor size (Fig. 6A) in mice treated with GLA (20 mg/kg) was significantly lower than that of vehicle group. Compared with the vehicle group, the tumor volume grew slowly in GLA group (Fig. 6B). The average tumor weight was 3.73 ± 0.68 g for the control group, and 1.71 ± 0.42 g for GLA (20 mg/kg) group (Fig. 6C). In the histological level, cell proliferation and microvessel density were evaluated through Ki-67 and CD31, respectively. GLA markedly suppressed the expressions of Ki-67 and CD31 in subcutaneous tumor tissue (Fig. 6D).

Discussion

Bladder cancer is characterized by high rate of recurrence, progression, and mortality. It is urgent to identify the underlying molecular mechanisms and develop a novel anti-tumor therapy for bladder cancer. GLA has been reported as a potential agent to treat some specific cancers [3]. In this study, we demonstrated for the first time that GLA inhibited the proliferation of human bladder cell lines UMUC3 (p53 wild-type), HT1197 (p53 wild-type), T24(p53 mutant type), J82(p53 mutant type), in a time- and dose-dependent manner by CCK-8 assay [12].

The cell cycle progresses sequentially through four phases, including G0/G1, S, G2 and M. Cell cycle dysregulation is one of the most frequent alterations during tumor development [13] and blockade of the cell cycle progression is considered as an effective strategy to eliminate cancer cells [14]. GLA has been found to arrest the liver cancer cells at the G2/M stage of the cell cycle [15]. Our data from flow cytometry showed that the proportion of G2/M cells increased dose-dependently, suggesting that GLA induced G2/M arrest in UMUC3 cells. GLA-induced G2/M arrest may help UMUC3 cells to properly repair DNA

defects, thus preventing their transmission to the resulting daughter cells. CDK1 (also known as Cdc2) activity requires binding of regulatory subunit named Cyclin B1 and the activation of Cyclin B1/CDK1 complex is responsible for the transition from the G2 to M phase [16]. At the G2/M transition, the phosphatase Cdc25C activates Cyclin B1/CDK1 by dephosphorylation of Thr14 and Tyr15 in CDK1 [17]. The CDK inhibitor $p21^{Waf1/Cip1}$ inactivates Cyclin B1/CDK1 complex in p53-dependent sustained G2/M arrest [18]. We next demonstrated that GLA treatment upregulated the protein level of $p21^{Waf1/Cip1}$ but downregulated Cyclin B1, CDK1, and Cdc25C, providing a molecular-level explanation for GLA-induced G2/M arrest in UMUC3 cells. Previous studies have investigated microtubule stabilizing agents such as paclitaxel, docetaxel, which ultimately alter the equilibrium between tubulin and microtubule resulting in disruption of the mitotic spindle, thereby effecting a critical transition in the cell cycle, leading to cell death [19]. In this study, we couldn't prove that GLA has a specific relationship with microtubules in inhibiting cell cycle.

Apoptosis is a type of programmed cell death characterized by such morphological changes as cell shrinkage, nuclear fragmentation, chromatin condensation. Inducing apoptosis in cancer cells is one of the most important markers of cytotoxic anti-tumor agents [19]. We observed dose-dependent induction of apoptosis in UMUC3 cells following GLA treatment. Apoptosis can be initiated by either death receptors (extrinsic) pathway or mitochondria (intrinsic). Many natural compounds have been found to induce apoptosis through the intrinsic pathway [20]. The Bcl-2 family proteins are known as key regulators of apoptosis, including anti-apoptotic members (e.g. Bcl-2 and Bcl-xL) and pro-apoptotic members (e.g. Bax and Bad). An elevated Bax/Bcl-2 ratio causes a release of cytochrome c (Cyt-C) from mitochondria to the cytosol where it activates Caspase-9. Subsequently, the active Caspase-9 can activate Caspase-3, an effector caspase that cleaves PARP at the onset of apoptosis [21]. Western blotting analysis showed that GLA treatment downregulated the protein expression of Bcl-2 whereas upregulated the level of Bax, Cleaved Caspase-9, Cleaved Caspase-3 and Cleaved PARP. Moreover, immunofluorescence staining confirmed that both cytoplasmic and nuclear expressions of Cleaved Caspase-3 were significantly enhanced after GLA treatment. Although active Caspase-3 has been detected not only in the cytoplasm and mitochondria but also in the nuclear fraction of apoptotic cells, the precise molecular mechanism of its nuclear translocation remains unknown [22].

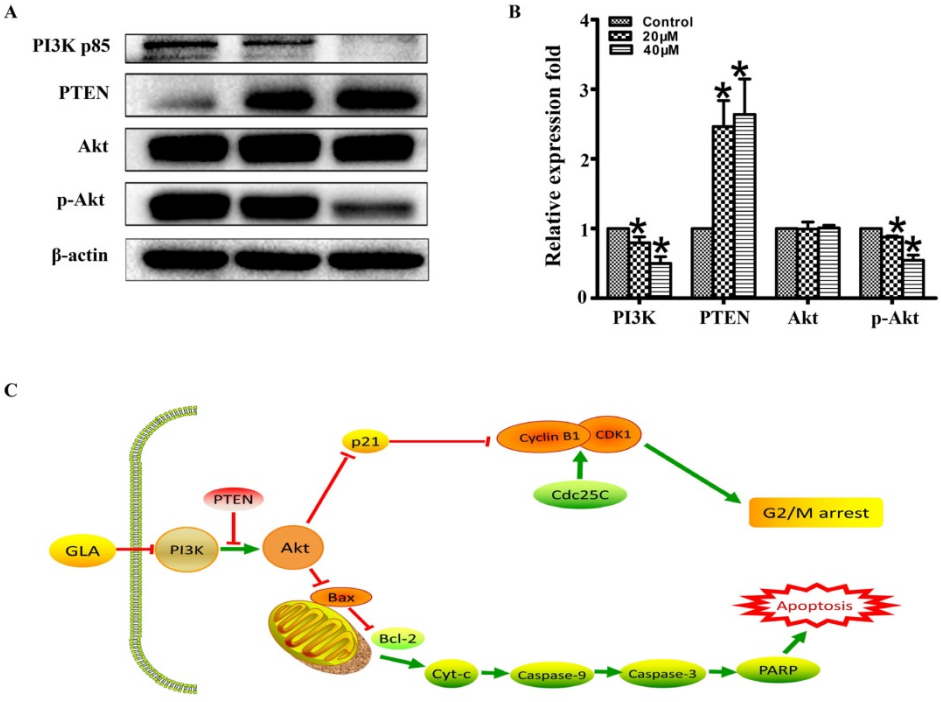

Figure 5. GLA inhibits the PI3K/Akt pathway in UMUC3 cells. (A, B) UMUC3 cells were treated with GLA (0, 20 and 40 μM) for 24 h. Proteins were extracted and western blotting was then performed to analyze the expressions of PI3K p85, PTEN, Akt, p-Akt (Ser473) are expressed as the mean ± S.D. from three independent experiments. *$P < 0.05$ vs. the control group. **(C)** Scheme of the proposed mechanism for GLA-induced G2/M arrest and apoptosis in UMUC3 cells. Red arrows represent inhibition of the next signal while green arrows represent the promotion of the next signal.

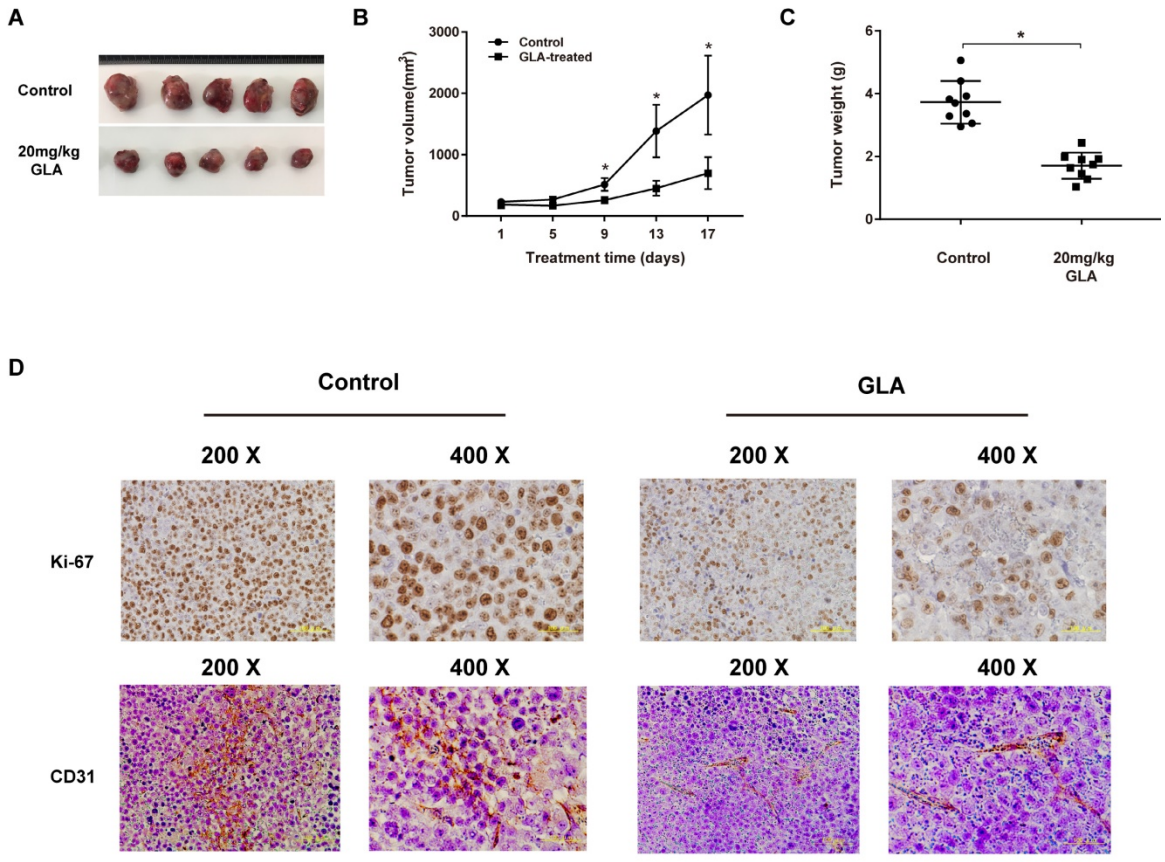

Figure 6. GLA exhibits the anti-tumor effect on UMUC3 cells in vivo. (A) The UMUC3 tumors from mice were excised and photographed after two-week treatment. **(B)** Tumor growth curves in mice injected with UMUC3 cells at the indicated days. **(C)** The average weight of excised tumors from treatment group significantly decreased compared with vehicle treatment. **(D)** Immunohistochemistry analysis of Ki-67 and CD31 expressed in harvested tumor tissues. Data are expressed as the mean ± S.D. (n = 9). *P < 0.05 vs. the control group.

Increasing evidence suggest that the PI3K/Akt pathway involves the pathogenesis of many cancers and regulates various cellular processes including differentiation, proliferation, metastasis, and metabolism [23]. PI3Ks are categorized into three classes (I, II and III) and the class I PI3Ks includes two subgroups, IA and IB. The extensively studied class IA PI3K, a heterodimer consisting of a p85 regulatory subunit and a p110 catalytic subunit, plays a key role in tumorigenesis, which will be only discussed here [24]. Activation of PI3K converts PI (3, 4) P2 to PI (3, 4, and 5) P3, which can be reversed by PTEN. PIP3, as a second messenger, recruits Akt to the plasma membrane where Akt is phosphorylated at Thr308 and Ser473 [25]. The activated Akt may promote cell cycle progression and tumor growth through its downstream p53 pathway and Bcl-2 family proteins. Akt phosphorylates mouse double minute 2 (MDM2), an E3 ubiquitin ligase that triggers p53 degradation [26]. The tumor suppressor gene p53 induces cell cycle arrest and apoptosis by increasing the expressions of its two transcriptional targets $p21^{Waf1/Cip1}$ and Bax, respectively [27]. The PI3K/Akt pathway is considered to play a major role in bladder carcinogenesis, but specific mechanisms remain to be investigated [28]. As shown in Figure 5C, we proposed the molecular mechanism for GLA-induced G2/M arrest and apoptosis in UMUC3 cells. Following GLA treatment, the levels of PI3K p85 subunit and the phosphorylation of Akt at Ser473 site were downregulated while the levels of PTEN were upregulated. The location of p-Akt (Ser473) expression was also determined by immunofluorescence staining. Consistent with in vitro experiments, GLA treatment (20 mg/kg) for 14 days exhibited a significant anti-tumor effect in UMUC3 tumor xenograft of NOD/SCID mice model. As a good immunohistochemical marker of proliferation, Ki-67 is related to the traditional prognostic factors of grade, stage and recurrence in superficial urothelial cancer [29]. Interestingly, we also detected the decreased expression of Ki-67 in tumor tissue.

To our knowledge, this is the first report to demonstrate the anti-neoplastic effect of GLA on human bladder cancer. However, it should be noted that the poor solubility of GLA in water poses serious obstacles to its practical use as a therapeutic agent for bladder cancer. GLA nanosuspensions both in vitro

and in vivo have recently been demonstrated to achieve a better anti-tumor efficacy compared with the free-drug group, which may contribute to the wider use of GLA for future research [7]. Further studies on metastatic characteristics of bladder cancer are also needed to better understand the therapeutic potential of GLA.

In conclusion, our observations demonstrate that GLA induced G2/M cell cycle arrest and apoptosis of bladder cancer UMUC3 cells via suppression of the PI3K/Akt signaling pathway. Therefore, we believe that GLA may be developed into a novel and effective therapeutic agent targeting the PI3K/Akt pathway in bladder cancer.

Acknowledgements

This study was funded by grants from the Science and Technology Planning Project of the Guangdong Province (2016A020215109), the Guangdong Natural Science Foundation (No. 2015A03031 3291) and the Ministry of Education, Culture, Sports, Science and Technology of Japan (No. 17K11138).

Competing Interests

The authors have declared that no competing interest exists.

References

1. Zhang Y, Sha D, Sha M, Yuan C. Determination of glaucocalyxin A in the leaves of Plectranthus japonicus (Burm.) Koidz. var. glaucocalyx (Maxim.) Koidz. by HPLC. Zhongguo Zhong yao za zhi= Zhongguo zhongyao zazhi= China journal of Chinese materia medica. 1991; 16: 679-80.
2. Jin Y, Gui M, Wang B. Studies on chemical constituents in the roots of Rabdosia japonica (Burm. f). Hara var. glaucocalyx (Maxin) Hara. Zhongguo Zhong yao za zhi= Zhongguo zhongyao zazhi= China journal of Chinese materia medica. 2000; 25: 678-9.
3. Xiang Z, Wu X, Liu X, Jin Y. Glaucocalyxin A: a review. Natural product research. 2014; 28: 2221-36.
4. Gao LW, Zhang J, Yang WH, Wang B, Wang JW. Glaucocalyxin A induces apoptosis in human leukemia HL-60 cells through mitochondria-mediated death pathway. Toxicology in vitro. 2011; 25: 51-63.
5. Li M, Jiang X-G, Gu Z-L, Zhang Z-B. Glaucocalyxin A activates FasL and induces apoptosis through activation of the JNK pathway in human breast cancer cells. Asian Pacific Journal of Cancer Prevention. 2013; 14: 5805-10.
6. Li W, Tang X, Yi W, Li Q, Ren L, Liu X, et al. Glaucocalyxin A inhibits platelet activation and thrombus formation preferentially via GPVI signaling pathway. PloS one. 2013; 8: e85120.
7. Han M, Li Z, Guo Y, Zhang J, Wang X. A nanoparticulate drug-delivery system for glaucocalyxin A: formulation, characterization, increased in vitro, and vivo antitumor activity. Drug delivery. 2016; 23: 2457-63.
8. Siegel RL, Miller KD, Fedewa SA, Ahnen DJ, Meester RG, Barzi A, et al. Colorectal cancer statistics, 2017. CA: a cancer journal for clinicians. 2017; 67: 177-93.
9. Kamat AM, Hahn NM, Efstathiou JA, Lerner SP, Malmström P-U, Choi W, et al. Bladder cancer. The Lancet. 2016; 388: 2796-810.
10. Huang P, Chen J, Wang L, Na Y, Kaku H, Ueki H, et al. Implications of transcriptional factor, OCT-4, in human bladder malignancy and tumor recurrence. Medical Oncology. 2012; 29: 829-34.
11. Dy GW, Gore JL, Forouzanfar MH, Naghavi M, Fitzmaurice C. Global burden of urologic cancers, 1990–2013. European urology. 2017; 71: 437-46.
12. Zhang X, Liu D, Hayashida Y, Okazoe H, Hashimoto T, Ueda N, et al. G Protein-Coupled Receptor 87 (GPR87) Promotes Cell Proliferation in Human Bladder Cancer Cells. International journal of molecular sciences. 2015; 16: 24319-31.
13. Li X, Xu P, Wang C, Xu N, Xu A, Xu Y, et al. Synergistic effects of the immune checkpoint inhibitor CTLA-4 combined with the growth inhibitor lycorine in a mouse model of renal cell carcinoma. Oncotarget. 2017; 8: 21177.
14. Otto T, Sicinski P. Cell cycle proteins as promising targets in cancer therapy. Nature Reviews Cancer. 2017; 17: 93-115.
15. Wang C, Wang Q, Li X, Jin Z, Xu P, Xu N, et al. Lycorine induces apoptosis of bladder cancer T24 cells by inhibiting phospho-Akt and activating the intrinsic apoptotic cascade. Biochemical and biophysical research communications. 2017; 483: 197-202.
16. Malumbres M, Barbacid M. Cell cycle, CDKs and cancer: a changing paradigm. Nature Reviews Cancer. 2009; 9: 153-66.
17. Forester CM, Maddox J, Louis JV, Goris J, Virshup DM. Control of mitotic exit by PP2A regulation of Cdc25C and Cdk1. Proceedings of the National Academy of Sciences. 2007; 104: 19867-72.
18. Nakayama Y, Yamaguchi N. Role of cyclin B1 levels in DNA damage and DNA damage-induced senescence. International review of cell and molecular biology. 2012; 305: 303-37.
19. Tangutur AD, Kumar D, Krishna KV, Kantevari S. Microtubule Targeting Agents as Cancer Chemotherapeutics: An Overview of Molecular Hybrids as Stabilizing and Destabilizing Agents. Current topics in medicinal chemistry. 2017; 17: 2523-37.
20. Safarzadeh E, Shotorbani SS, Baradaran B. Herbal medicine as inducers of apoptosis in cancer treatment. Advanced pharmaceutical bulletin. 2014; 4: 421.
21. Yamada H, Abe T, Li S-A, Tago S, Huang P, Watanabe M, et al. N′-[4-(dipropylamino) benzylidene]-2-hydroxybenzohydrazide is a dynamin GTPase inhibitor that suppresses cancer cell migration and invasion by inhibiting actin polymerization. Biochemical and biophysical research communications. 2014; 443: 511-7.
22. Katiyar SK, Roy AM, Baliga MS. Silymarin induces apoptosis primarily through a p53-dependent pathway involving Bcl-2/Bax, cytochrome c release, and caspase activation. Molecular cancer therapeutics. 2005; 4: 207-16.
23. Kamada S, Kikkawa U, Tsujimoto Y, Hunter T. Nuclear translocation of caspase-3 is dependent on its proteolytic activation and recognition of a substrate-like protein (s). Journal of Biological Chemistry. 2005; 280: 857-60.
24. Guo K, Huang P, Xu N, Xu P, Kaku H, Zheng S, et al. A combination of YM-155, a small molecule survivin inhibitor, and IL-2 potently suppresses renal cell carcinoma in murine model. Oncotarget. 2015; 6: 21137.
25. Engelman JA, Luo J, Cantley LC. The evolution of phosphatidylinositol 3-kinases as regulators of growth and metabolism. Nature Reviews Genetics. 2006; 7: 606-19.
26. Ihle NT, Powis G. Inhibitors of phosphatidylinositol-3-kinase in cancer therapy. Molecular aspects of medicine. 2010; 31: 135-44.
27. Tu Y, Kim E, Gao Y, RANkIN GO, Li B, Chen YC. Theaflavin-3, 3'-digallate induces apoptosis and G2 cell cycle arrest through the Akt/MDM2/p53 pathway in cisplatin-resistant ovarian cancer A2780/CP70 cells. International journal of oncology. 2016; 48: 2657-65.
28. Chen D, Tavana O, Chu B, Erber L, Chen Y, Baer R, et al. NRF2 Is a Major Target of ARF in p53-Independent Tumor Suppression. Molecular cell. 2017; 68: 224-32. e4.
29. Sathe A, Nawroth R. Targeting the PI3K/AKT/mTOR Pathway in Bladder Cancer. Urothelial Carcinoma: Springer; 2018; 1655:335-50.